605

Analysis of stiffened plates composed by different materials by the boundary element method

Gabriela R. Fernandes[*] and João R. Neto

Civil Engineering Department, Federal University of Goiás (UFG), CAC, Av. Dr. Lamartine Pinto de Avelar, 1120, Setor Universitário, CEP 75700-000 Catalão, GO, Brazil

Abstract. A formulation of the boundary element method (BEM) based on Kirchhoff's hypothesis to analyse stiffened plates composed by beams and slabs with different materials is proposed. The stiffened plate is modelled by a zoned plate, where different values of thickness, Poisson ration and Young's modulus can be defined for each sub-region. The proposed integral representations can be used to analyze the coupled stretching-bending problem, where the membrane effects are taken into account, or to analyze the bending and stretching problems separately. To solve the domain integrals of the integral representation of in-plane displacements, the beams and slabs domains are discretized into cells where the displacements have to be approximated. As the beams cells nodes are adopted coincident to the elements nodes, new independent values arise only in the slabs domain. Some numerical examples are presented and compared to a well-known finite element code to show the accuracy of the proposed model.

Keywords: plate bending; boundary elements; stiffened plates; membrane effects; stretching problem

1. Introduction

The boundary element method (BEM) has already proved to be a suitable numerical tool to deal with plate bending problems. It is particularly recommended for the analysis of building floor structures where the combinations of slab, beam and column elements can be more accurately represented, considering that the method is very accurate to compute the effects of concentrated (in fact loads distributed over small areas) and line loads, as well to evaluate high gradient values as bending and twisting moments, and shear forces. Moreover, the same order of errors is expected when computing deflections, slopes, moments and shear forces, because the tractions are not obtained by differentiating approximation function as for other numerical techniques. In this context, it is worth also mentioning two edited books (Beskos 1991, Aliabadi 1998) containing BEM formulations applied to plate bending showing several important applications in the engineering context.

The direct BEM formulation applied to Kirchhoff's plates has appeared in the seventies (Bezine 1978, Stern 1979 and Tottenhan 1979). Besine (1981) apparently was the first to use a boundary element to analyse building floors structures by analysing plates with internal point

---

*Corresponding author, Ph.D., E-mail: gabrielar.fernandes@gmail.com

supports. It is interesting mentioning the works Hu and Hartley (1994), Hartley (1996), Tanaka and Bercin (1997) where BEM was coupled with FEM to develop the numerical model. In these works boundary elements have been chosen to model the plate behaviour, while beams and columns have been represented by finite elements. As usual, the different elements are combined together by enforcing equilibrium and compatibility conditions along the interfaces. However, for complex floor structures the number of degrees of freedom may increase rapidly diminishing the solution accuracy.

In Tanaka *et al*. (2000), Sapountzakis and Katsikadelis (2000a, b), Paiva and Aliabadi (2004), are proposed BEM formulations for analysing the bending problem of beam-stiffened elastic plates. A BEM formulation for building floor structures in which the eccentricity effects are considered and the warping influence arising from both shear forces and twisting moments is taken into account is presented by Sapountzakis and Mokos (2007). In Venturini and Waidemam (2009a, b) develop BEM formulations for elastoplastic analysis of reinforced plates and in Venturini and Waidemam (2010) the same authors extend the previous formulation for considering geometric non-linearity as well. Wutzow *et al*. (2006) present a non-linear BEM formulation for analysing reinforced porous materials, where the beam elements are modelled by the Reissner's theory applied to shell elements.

An alternative scheme to reduce the number of degrees of freedom has been proposed by Fernandes and Venturini (2002) to perform simple bending analysis using only a BEM formulation based on Kirchhoff's hypothesis. In this work the building floor is modelled by a zoned plate where each sub-region defines a beam or a slab, being all of them represented by their middle surface. The beams are modelled as narrow sub-regions with larger thickness, being the tractions eliminated along the interfaces, reducing therefore the total number of unknowns. Then in order to reduce further the degrees of freedom, the displacements are approximated along the beam width, leading to a model where the bending values are defined only on the beams axis and on the plate boundary without beams. This composed structure is treated as a single body, being the equilibrium and compatibility conditions automatically taken into account. In Fernandes and Venturini (2005) the authors have extended the formulation proposed in Fernandes and Venturini (2002) in order to represent all sub-regions by a same reference surface, so that the eccentricity effects should be taken into account. It is important to note that in the formulations proposed in Fernandes and Venturini (2002, 2005) all sub-regions should have the same Poisson's ration and Young's modulus. In Fernandes and Venturini (2007) the same authors have extended the BEM linear formulation presented in Fernandes and Venturini (2005) in order to perform the non-linear analysis of stiffened plates and in Fernandes *et al*. (2010) columns have been incorporated to the formulation developed in Fernandes and Venturini (2005). A BEM formulation for simple bending analysis of stiffened plates composed by different materials is proposed in Fernandes (2009) whose formulation is an extension of the one developed in Fernandes and Venturini (2002). As in the formulation proposed in Fernandes (2009) there is no domain integrals involving displacements the number of degrees of freedom remain the same.

In this work the formulation presented in Fernandes and Venturini (2005) for the coupled stretching-bending analysis is now extended to consider the stiffened plate with different materials. The sub-regions can be defined with different values of Poisson's ration and Young's modulus, but these values have to be constant over each sub-region. The proposed integral representations can be also used to analyse the bending and stretching problems separately without coupling them. In order to compute the domain integrals of the integral representation of in-plane displacements (related to the stretching problem) the beams and slabs domains had to be

discretized into cells, considering different approximations for the displacements over the beams and slabs domains. For the beams, the displacements over the domain are written in terms of their nodal values defined along the beam axis which are already required to approximate the displacements over the elements. Thus, new independent values have to be defined only in the slabs domain. The accuracy of the proposed model is confirmed by numerical examples whose results are compared with a well-known finite element code.

2. Basic equations

Without loss of generality, let us consider the stiffened plate depicted in Fig. 1(a), where t_1, t_2 and t_3 are the thicknesses of the sub-regions Ω_1, Ω_2 and Ω_3, whose external boundaries are Γ_1, Γ_2 and Γ_3, respectively. In Fig. 1(a) the total external boundary is given by Γ while Γ_{jk} represents the interface between the adjacent sub-regions Ω_j and Ω_k. In the simple bending analysis all sub-regions are represented by their middle surface, as shown in Fig. 1(c), while for the coupled stretching-bending problem the Cartesian system of co-ordinates (axes x_1, x_2 and x_3) is defined on a chosen reference surface (see Fig. 1(b)), whose distance to the sub-regions middle surfaces are given by c_1, c_2 and c_3. As in Fig. 1(b) the reference surface is adopted coincident to Ω_2 middle surface one has $c_2=0$.

(a) plate surface view

(b) sub-regions represented by the reference surface   (c) sub-regions represented by their middle surfaces
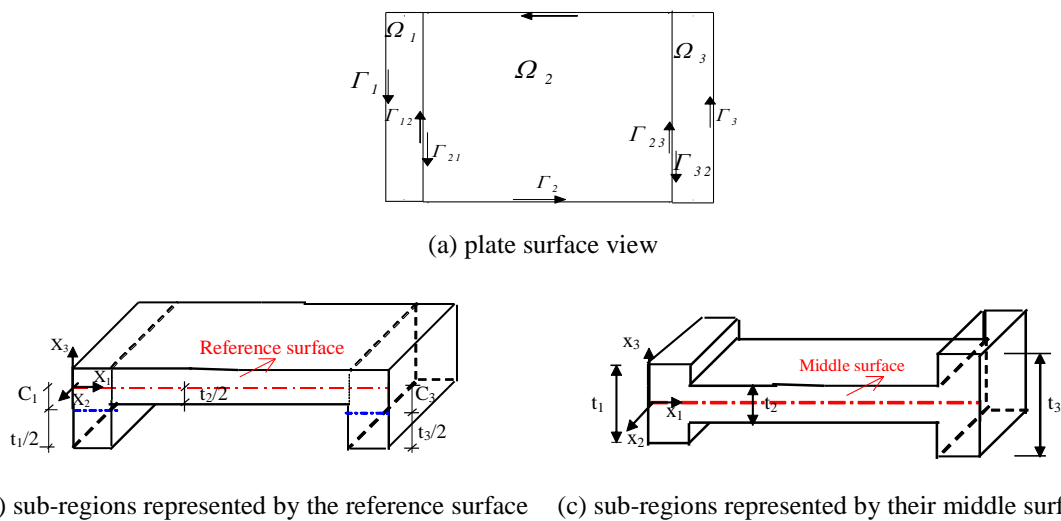
Fig. 1 Reinforced plate

Initially the bending and stretching problems will be treated separately in order to present their equilibrium equations and their internal force×displacement relations as well. Then in section 3 the two problems will be coupled in order to obtain the bending problem solution taking into account the membrane effects. Let us consider initially the bending problem. For a point placed at any of those plate sub-regions, the following equations can be defined:

-Equilibrium equations in terms of internal forces:

$$\text{m}_{ij},_j - q_i = 0 \tag{1}$$

$$q_i,_i + g = 0 \tag{2}$$

where g is the distributed load acting on the plate middle surface, m_{ij} are bending and twisting moments and q_i represents shear forces, with subscripts taken in the range $i,j=\{1, 2\}$.

-The plate bending differential equation

$$m_{ij,ij} + g = 0 \tag{3}$$

or

$$w,_{iijj} = g / D \qquad (i, j = 1,2) \tag{4}$$

where $D=Et^3/(1-v^2)$ is the flexural rigidity, E the Young's modulus, v the Poisson's ratio and $w,_{iijj}=\nabla^4 w$, being ∇^4 the bi-harmonic operator.

- The generalised internal force×displacement relations

$$m_{ij} = -D\left(v\delta_{ij}w,_{kk} + (1-v)w\,,_{ij}\right) \qquad i,j=1, 2 \tag{5}$$

$$q_i = -Dw,_{jji} \tag{6}$$

where δ_{ij} is the Kronecker delta.

- The effective shear force

$$V_n = q_n + \partial m_{ns} / \partial s \tag{7}$$

where (n, s) are the local co-ordinate system, with n and s referred to the plate boundary normal and tangential directions, respectively.

Considering now the stretching problem, the in-plane equilibrium equation is

$$N_{ij},_j + b_i = 0 \qquad i, j=1, 2 \tag{8}$$

where b_i are body forces distributed over the plate middle surface and N_{ij} is the membrane internal force, which, for plane stress conditions, can be written in terms of the in-plane deformations ε_{ij}^S as follows

$$N_{ij} = \frac{\overline{E}}{(1-v^2)}\left[v\,\varepsilon_{kk}^S \delta_{ij} + (1-v)\varepsilon_{ij}^S\right] \tag{9}$$

where $\overline{E} = Et$.

For the coupled stretching-bending problem, the strain and stress components are the sum of an uniform part due to stretching plus a non-uniform part due to bending, i.e.

$$\varepsilon_{ij} = \varepsilon_{ij}^S + \varepsilon_{ij}^B \tag{10a}$$

$$\sigma_{ij} = \sigma_{ij}^S + \sigma_{ij}^B \tag{10b}$$

where B and S refer, respectively to bending and stretching problems; $\varepsilon_{ij}^{B} = -x_3 w,_{ij}$ with $w,_{ij}$ being the plate surface curvature.

The coupled stretching-bending problem definition is then completed by assuming the following boundary conditions over Γ: $U_i = \bar{U}_i$ on Γ_u (generalised displacements: deflections and rotations (bending problem); in-plane displacements (stretching problem)) and $P_i = \bar{P}_i$ on Γ_p (generalised tractions: bending moments and effective shear forces (bending problem); in-plane tractions (stretching problem)), where $\Gamma_u \cup \Gamma_p = \Gamma$. Note that the integral representations derived in section 3 can be also used to analyse the simple bending or the stretching problem without coupling thee two problems. For that we have only to consider c_m null (see Fig. 1) for all sub-regions (where m varies from 1 to the sub-regions number).

3. Integral representations

In this section, we are going to derive the integral representations of displacements for the simple bending problem, the stretching problem and the coupled stretching-bending problem of a zoned plate where the thickness, Poisson's ratio and Young's modulus may vary from one sub-region to another, but must be constant over each sub-region. The equations will be derived by applying the reciprocity theorem to each sub-region and summing them to obtain the equation for the whole body. Complementary domain integral terms will be inserted in the reciprocity relation to take into account variations of material properties or rigidities from one sub-region to another as well as the effects of the relative position of the sub-region middle surfaces. The integral equations derived in this section can be used to model building floor structures, being each sub-region the representation of either a slab or a beam. Note that if the coupled stretching-bending problem is considered, in the final displacements representations all sub-regions will be represented by their reference surface, as depicted in Fig. 1(b). If the two problems are not coupled the sub-regions are represented by their middle surface (c_m is null for all sub-regions *m, see* Fig. 1) and the integral representations can be used to analyse the bending problem or the stretching problem separately.

As described in details in Fernandes and Venturini (2005), from Betti's theorem, the following two equations can be obtained for any sub-region Ω_m, respectively, for the bending and stretching problems

$$\int_{\Omega_m} \varepsilon_{ijk}^{Sm*} N_{jk}^{m} d\Omega = \int_{\Omega_m} N_{ijk}^{m*} \varepsilon_{jk}^{Sm} d\Omega \qquad\qquad \text{i, j, k=1, 2} \qquad\qquad \text{(11a)}$$

$$\int_{\Omega_m} w,_{jk}^{m*} m_{jk}^{m} d\Omega = \int_{\Omega_m} m_{jk}^{m*} w,_{jk}^{m} d\Omega \qquad\qquad \text{j, k=1, 2} \qquad\qquad \text{(11b)}$$

where ε_{ijk}^{Sm*}, N_{ijk}^{m*}, $w,_{jk}^{m*}$ and m_{jk}^{m*} are fundamental solutions.

Note that for Eq. (11b) the unit load is applied in x_3 direction. Eqs. (11) can be now modified by writing the fundamental strains of sub-region Ω_m in terms of the values (ε_{ijk}^{S*}, $w,_{jk}^{*}$, D and $\bar{\bar{E}}$ t) referred to the sub-region where the load point s is placed. This simplifies the formulation because allows to eliminate the tractions along the interfaces. Thus, the following relations can be

defined

$$\varepsilon_{ijk}^{Sm*} = \varepsilon_{ijk}^{S*} \overline{E} / \overline{E}_m \tag{12}$$

$$w_{,jk}^{m*} = [D / D_m] w_{,jk}^{*} \tag{13}$$

where $\overline{E}_m = E_m t_m$, being E_m the Young's modulus in the sub-region Ω_m.

Considering Eqs. (12) and (13) the moment m_{ij}^{m*} and the membrane force N_{ij}^{m*} can be also written in terms of v, m_{ij}^{*} and N_{ij}^{*} referred to the sub-region where the load point is placed as follows

$$m_{jk}^{*(m)} = \frac{v_m}{v} m_{jk}^{*} + D\left(\frac{v_m}{v} - 1\right) w_{,jk}^{*} \tag{14}$$

$$N_{ijk}^{*(m)} = \frac{\left(1 - v^2\right) v_m}{\left(1 - v_m^2\right) v} N_{ijk}^{*} + \frac{\overline{E}}{\left(1 - v_m^2\right)}\left(1 - \frac{v_m}{v}\right) \varepsilon_{ijk}^{S*} \tag{15}$$

Replacing (14) and (13) into Eq. (11b) as well as Eq. (12) and (15) into (11a) one obtains, respectively, for the bending and stretching problems

$$\int_{\Omega_m} w_{,jk}^{*} m_{jk} d\Omega_m = \frac{D_m v_m}{D v} \int_{\Omega_m} w_{,jk} m_{jk}^{*} d\Omega_s + D_m\left(\frac{v_m}{v} - 1\right) \int_{\Omega_m} w_{,jk} w_{,jk}^{*} d\Omega_m \tag{16}$$

$$\int_{\Omega_m} \varepsilon_{ijk}^{*S} N_{jk} d\Omega_m = \frac{\overline{\overline{E}}_m}{\overline{\overline{E}}} \frac{v_m}{v} \left[\int_{\Omega_m} \varepsilon_{jk}^{S} N_{ijk}^{*} d\Omega\right] + \overline{\overline{E}}_m\left(1 - \frac{v_m}{v}\right) \int_{\Omega_m} \varepsilon_{jk}^{S} \varepsilon_{ijk}^{*S} d\Omega_m \tag{17}$$

where $\overline{\overline{E}}_m = \dfrac{\overline{E}_m}{\left(1 - v_m^2\right)}$.

Note that in the case of having $v=0$, Eqs. (16) and (17) can't be used. On the other hand one can demonstrate that if $v=0$, Eq. (11) result into the same equations presented in Fernandes and Venturini (2005) related to the formulation where all sub-regions must have the same Poisson's ratio and Young's modulus. Applying Eqs. (16) and (17) for all sub-regions one obtains the following relations for the whole plate, respectively, for the bending and stretching problem

$$\int_{\Omega} w_{,jk}^{*} m_{jk} d\Omega = \sum_{m=1}^{N_S}\left[\frac{D_m v_m}{D v} \int_{\Omega_m} w_{,jk} m_{jk}^{*} d\Omega_m + D_m\left(\frac{v_m}{v} - 1\right) \int_{\Omega_m} w_{,jk} w_{,jk}^{*} d\Omega_m\right] \tag{18}$$

$$\int_{\Omega_m} \varepsilon_{ijk}^{*S} N_{jk} d\Omega_m = \sum_{m=1}^{N_S}\left[\frac{\overline{\overline{E}}_m}{\overline{\overline{E}}} \frac{v_m}{v} \int_{\Omega_m} \varepsilon_{jk}^{S} N_{ijk}^{*} d\Omega + \overline{\overline{E}}_m\left(1 - \frac{v_m}{v}\right) \int_{\Omega_m} \varepsilon_{jk}^{S} \varepsilon_{ijk}^{*S} d\Omega_m\right] \tag{19}$$

where N_s is the sub-regions number.

Eqs. (18) and (19) are the reciprocity relations of a stiffened plate composed by different materials, treating the bending and stretching problems separately, i.e., with all values related to the sub-regions middle surface. In the coupled stretching-bending problem, the boundary and interface values are referred to the reference surface (see Fig. 1). Therefore, to derive the reciprocity relations in which stretching and bending effects are coupled, we have to take into account the effects of the relative position of the sub-region middle surfaces. It is worth noting that internal normal forces and the curvatures do not depend on the plate surface position and therefore the local values are replaced by the global ones, i.e., $N_{jk}^m = N_{jk}$ and $w,_{jk}^m = w,_{jk}$. On the other hand, the in-plane strain and the bending moments change if the position of the plate surface is modified. Thus according to Eqs. (10) we can write strain and moment values of sub-region Ω_m (ε_{jk}^{Sm} and m_{jk}^m) in terms of the reference surface values (ε_{jk}^S and m_{jk}), as follows

$$\varepsilon_{jk}^{Sm} = \varepsilon_{jk}^S - c_m w,_{jk} \qquad\qquad \text{j, k = 1, 2} \qquad\qquad (20a)$$

$$m_{jk}^m = m_{jk} - c_m N_{jk} \qquad\qquad (20b)$$

where c_m is the distance from the reference surface to the middle surface of sub-region m (see Fig. 1 for more details).

Replacing Eq. (20a) into (19) and (20b) into (18) one obtains the following reciprocity relations for the coupled stretching-bending problem

$$\int_\Omega w,_{jk}^* m_{jk} d\Omega - \sum_{m=1}^{N_S} \int_{\Omega_m} c_m w,_{jk}^* N_{jk} d\Omega_m =$$

$$= \sum_{m=1}^{N_S} \left[\frac{D_m \nu_m}{D \nu} \int_{\Omega_m} w,_{jk} m_{jk}^* d\Omega_m + D_m \left(\frac{\nu_m}{\nu} - 1 \right) \int_{\Omega_m} w,_{jk} w,_{jk}^* d\Omega_m \right] \qquad (21)$$

$$\int_\Omega \varepsilon_{ijk}^{*S} N_{jk} d\Omega = \sum_{m=1}^{N_S} \frac{\bar{\bar{E}}_m}{\bar{\bar{E}}} \frac{\nu_m}{\nu} \left[\int_{\Omega_m} \varepsilon_{jk}^{2D} N_{ijk}^* d\Omega - c_m \int_{\Omega_m} w,_{jk} N_{ijk}^* d\Omega \right] +$$

$$+ \sum_{m=1}^{N_S} \bar{\bar{E}}_m \left(1 - \frac{\nu_m}{\nu} \right) \left[\int_{\Omega_m} \varepsilon_{jk}^S \varepsilon_{ijk}^{*S} d\Omega_m - c_m \int_{\Omega_m} w,_{jk} \varepsilon_{ijk}^{*S} d\Omega \right] \qquad (22)$$

Eq. (21) can be integrated by parts twice to give the following representation of deflection

$$k(s)w(s) = \sum_{m=1}^{N_S} \frac{D_m \nu_m}{D \nu} \int_{\Gamma_m} \left(M_n^* w,_n - V_n^* w \right) d\Gamma + \sum_{j=1}^{N_{int}} \int_{\Gamma_{ja}} \left(\frac{D_j \nu_j - D_a \nu_a}{D \nu} \right) \left(M_n^* w,_n - V_n^* w \right) d\Gamma_{ja} +$$

$$- \sum_{i=1}^{N_{c0}} \frac{D_i \nu_i}{D \nu} R_{ci}^* w_{ci} - \left(\frac{D_j \nu_j - D_a \nu_a}{D \nu} \right) \sum_{j=1}^{N_{c1}+N_{c2}} R_{cj}^* w_{cj} + \sum_{i=1}^{N_c} R_{ci} w_{ci}^* + \int_\Gamma \left(V_n w^* - M_{nn} w,_n^* \right) d\Gamma +$$

$$+\sum_{m=1}^{N_S} D_m\left(\frac{\nu_m}{\nu}-1\right)\int_{\Gamma_m}\left(w,_n\ w,_{nn}^*+w\left(\frac{Q_n^*}{D}-\frac{\partial w,_{ns}^*}{\partial s}\right)\right)d\Gamma+$$

$$+\sum_{j=1}^{N_{int}}\left[D_j\left(\frac{\nu_j}{\nu}-1\right)-D_a\left(\frac{\nu_a}{\nu}-1\right)\right]\int_{\Gamma_{ja}}\left(w,_n\ w,_{nn}^*+w\left(\frac{Q_n^*}{D}-\frac{\partial w,_{ns}^*}{\partial s}\right)\right)d\Gamma+$$

$$-\sum_{i=1}^{Nc0} D_i\left(\frac{\nu_i}{\nu}-1\right)R_{ci}^{*'}w_{ci}-\sum_{i=1}^{Nc1+Nc2}\left[D_i\left(\frac{\nu_i}{\nu}-1\right)-D_a\left(\frac{\nu_a}{\nu}-1\right)\right]R_{ci}^{*'}w_{ci}$$

$$+\sum_{m=1}^{N_s} c_m\int_{\Gamma_m}\left[p_n w,_n^* + p_s w,_s^*\right]d\Gamma_m+\sum_{j=1}^{N_{int}}\left(c_j-c_a\right)\int_{\Gamma_{ja}}\left[p_n w,_n^*+p_s w,_s^*\right]d\Gamma_j+\int_{\Omega_g}\left(gw^*\right)d\Omega_g+$$

$$-\sum_{m=1}^{N_s} c_m\int_{\Omega_i}\left[b_n w,_n^*+b_s w,_s^*\right]d\Omega_m \tag{23}$$

where N_c is the total number of corners, N_{int} is the interfaces number, no summation is implied on n and s that are local normal and shear direction co-ordinates, respectively; Γ_m is the external boundary of sub-region Ω_m; Γ_{ja} represents an interface, being the subscript a referred to the adjacent sub-region to Ω_j; N_{c0}, N_{c1} and N_{c2} are numbers of corners between boundary elements, between interface elements and between interface and boundary elements, respectively (see more details in Fernandes and Venturini (2005)); Ω_g is the plate loaded area and $R_{ci}^{*'}=w,_{ns}^{*(+)}-w,_{ns}^{*(-)}$, being $w,_{ns}^{*(+)}$ the value of the curvature $w,_{ns}^*$ after the corner i and $w,_{ns}^{*(-)}$ the value of $w,_{ns}^*$ before the corner i; the free term $K(s)$ can assume several values depending on the position of the collocation point s (see more details in Fernandes and Venturini 2005).

Integrating now Eq. (22) by parts one obtains the following integral representations of in-plane displacements

$$\left[-c_r K_{w,_i}(s)w,_i(s)+K_{u_l}(s)u_i(s)\right]=-\sum_{m=1}^{N_s}\frac{\overline{\overline{E}}_m\nu_m}{\overline{\overline{E}}\nu}\int_{\Gamma}\left(u_n p_{kn}^*+u_s p_{ks}^*\right)d\Gamma+$$

$$-\sum_{j=1}^{N_{int}}\frac{\left(\overline{\overline{E}}_j\nu_j-\overline{\overline{E}}_a\nu_a\right)}{\overline{\overline{E}}\nu}\int_{\Gamma_{ja}}\left(u_n p_{kn}^*+u_s p_{ks}^*\right)d\Gamma_{ja}+\sum_{m=1}^{N_s}\frac{\overline{\overline{E}}_m\nu_m}{\overline{\overline{E}}\nu}\int_{\Gamma_m}c_m\left[p_{kn}^*w,_n+p_{ks}^*w,_s\right]d\Gamma$$

$$+\sum_{j=1}^{N_{int}}\frac{\left(\overline{\overline{E}}_j c_j\nu_j-\overline{\overline{E}}_a c_a\nu_a\right)}{\overline{\overline{E}}\nu}\int_{\Gamma_{ja}}\left(p_{kn}^*w,_n+p_{ks}^*w,_s\right)d\Gamma_{ja}+\int_{\Gamma}\left(u_{kn}^*p_n+u_{ks}^*p_s\right)d\Gamma+\int_{\Omega_b}\left(u_{kn}^*b_n+u_{ks}^*b_s\right)d\Omega$$

$$-\sum_{m=1}^{N_s}\overline{\overline{E}}_m\left(1-\frac{\nu_m}{\nu}\right)\int_{\Gamma_m}\left[u_n\varepsilon_{kn}^{*S}+u_s\varepsilon_{kns}^{*S}\right]d\Gamma+\sum_{M=1}^{N_s}\overline{\overline{E}}_m c_m\left(1-\frac{\nu_m}{\nu}\right)\int_{\Gamma_m}\left[w,_n\ \varepsilon_{kn}^{*S}+w,_s\ \varepsilon_{kns}^{*S}\right]d\Gamma+$$

$$-\sum_{j=1}^{N_{int}}\left[\overline{\overline{E}}_j\left(1-\frac{v_j}{v}\right)-\overline{\overline{E}}_a\left(1-\frac{v_a}{v}\right)\right]\int_{\Gamma_{ja}}\left[u_n\varepsilon_{kn}^{*S}+u_s\varepsilon_{kns}^{*S}\right]d\Gamma_{ja}$$

$$+\sum_{j=1}^{N_{int}}\left[\overline{\overline{E}}_jc_j\left(1-\frac{v_j}{v}\right)-\overline{\overline{E}}_ac_a\left(1-\frac{v_a}{v}\right)\right]\int_{\Gamma_{ja}}\left[w_{,n}\varepsilon_{kn}^{*S}+w_{,s}\varepsilon_{kns}^{*S}\right]d\Gamma_{ja}+$$

$$+\sum_{m=1}^{N_S}\overline{\overline{E}}_m\left(1-\frac{v_m}{v}\right)\int_{\Omega_m}u_j\varepsilon_{ijk,k}^{*S}d\Omega_m-\sum_{m=1}^{N_S}\overline{\overline{E}}_mc_m\left(1-\frac{v_m}{v}\right)\int_{\Omega_m}w_{,j}\varepsilon_{ijk,k}^{*S}d\Omega_m \qquad (24)$$

where $p_{ik}^*=N_{ik}^*$, with $k=n,s$, is the usual traction fundamental solutions for the stretching problem; the free term values are given in Fernandes and Venturini (2005); c_R is the distance of the collocation point sub-region to the reference surface.

Note that Eq. (24) can be used to analyse the stretching problem of plates without considering the bending problem and Eq. (23) can be used to analyse the bending problem without considering the membrane effects, which is the formulation developed in Fernandes (2009). For that we have only to consider the values c_m, c_a, c_r and c_j nulls in both equations. Eqs. (23) and (24) are the exact representations of deflection and in-plane displacements of a zoned plate for the coupled stretching-bending problem. In the set of equations, to be discussed in the next section, if the coupled stretching-bending problem is considered these equations have to be coupled and can't be treated separately. The interface values V_n and M_n were eliminated, remaining therefore four generalized displacements, w, $w_{,n}$; u_n and u_s and two in-plane tractions, p_n and p_s as unknown values along interfaces. Note that the tractions, p_n and p_s have been also eliminated on the interfaces for the stretching problem (Eq. (24)), but not for the bending problem (Eq. (23)). The rotation $w_{,s}$ is conveniently replaced by numerical derivatives of w, therefore leading to six unknowns at each interface node. On the external boundary eight values are defined: w, $w_{,n}$; u_n, u_s, p_n, p_s M_n and V_n, requiring therefore four equations for each boundary node. In Eq. (24) besides the problems values defined along the external boundary and interfaces one has also the values u_i and $w_{,i}$ defined inside the domain. Thus to solve the problem, the external boundary and interfaces must be discretized into elements and the domain into cells.

Observe that differentiating relation (23) once one can obtain the integral representation of deflection derivative as well as the in-plane displacements derivatives can be obtained by differentiating Eq. (24) and the membrane forces computed considering Eq. (8). Differentiating once more Eq. (23) to obtain the curvature integral representations at internal points and applying the definition given in Eq. (5) the bending and twisting moment integral representations can be derived. To obtain the shear force integral representation, completing the internal force values at internal points, one has to differentiate the curvature equation once and apply the definition given in Eq. (6).

Eqs. (23) and (24) can be used for solving the coupled stretching-bending problem of stiffened plates, but in this case the collocation points would have to be adopted on the interfaces and along all external boundary. However we have considered some approximations for the displacements over the beam cross sections in order to translate the displacement components related to the beam interfaces to its axis. In this model instead of having interface collocations points we have collocations points placed along the beams axis and along the part of the external boundary where

(a) Local system of coordinates on beams   (b) Tractions on internal beam interfaces
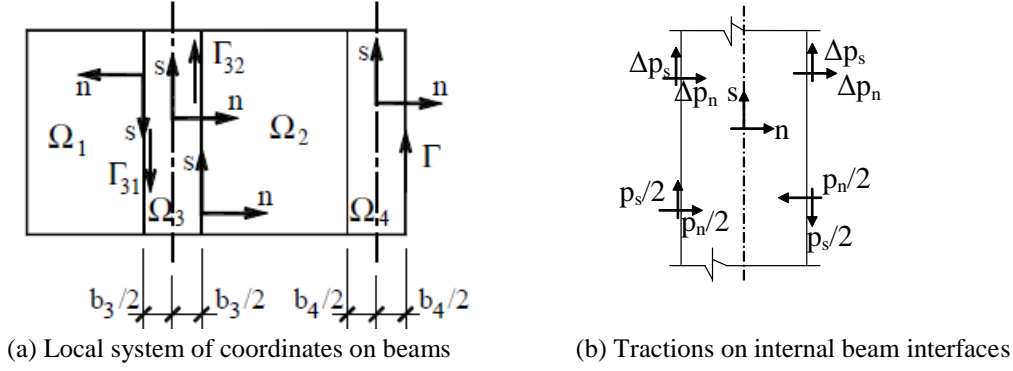
Fig. 2 Reinforced plate view

no beam is defined. These kinematics approximations are the same adopted in the formulation presented in Fernandes and Venturini (2005) applied to stiffened plates with v and E constant over all sub-regions. The deflection and in-plane displacements are assumed to vary linearly along the beam width, while the deflection normal derivative is adopted constant (see more details in Fernandes and Venturini 2005). Then, the displacement components related to the beam interfaces are written in terms of theirs values along the skeleton line, decreasing the number of degrees of freedom. Besides approximating the displacement field, one can also simplify conveniently the interface tractions to reduce the number of the required values by assuming linear distribution of stresses across the beam section. Let us consider the beam B_3 represented in Fig. 2(a) by the sub-region Ω_3. The tractions $p_k^{\Gamma_{31}}$ and $p_k^{\Gamma_{32}}$ along the interfaces Γ_{31} and Γ_{32}, can be conveniently split into two parts: Δp_k and p_k (related to the beam skeleton line), as follows (see Fig. 2 (b))

$$p_k^{\Gamma_{31}} = p_k / 2 + \Delta p_k \tag{25}$$

$$p_k^{\Gamma_{32}} = -p_k / 2 + \Delta p_k \tag{26}$$

The part of the tractions Δp_k is referred to linear stress field across the beam and is written in terms of displacement derivatives using Hooke's law, as follow

$$\Delta p_k = Gt\left[\frac{2v}{(1-v)}u_{\ell,\ell}\,n_k + (u_{k,n} + u_{n,k})\right] \qquad k=n,s \tag{27}$$

where the n is the beam axis outward vector and G the shear modulus.

The part p_k of Eqs. (25) and (26) refers to the constant stress distribution across the beam section and represents new independent values, i.e., new degrees of freedom for internal beams. Note that in Eq. (27) the displacements derivatives $u_{n,s}$ and $u_{s,s}$ with respect to beam axis, direction s, are replaced by numerical derivatives of u_n and u_s, respectively. Adopting these approximations for displacements and tractions, the number of values at each internal beam skeleton node remains eight: three displacements (w, u_n and u_s) three rotations ($w_{,n}$; $u_{n,n}$ and $u_{s,n}$) and two distributed forces (p_n and p_s). Therefore, for collocations defined along the internal beam axis one has to write eight different integral representations.

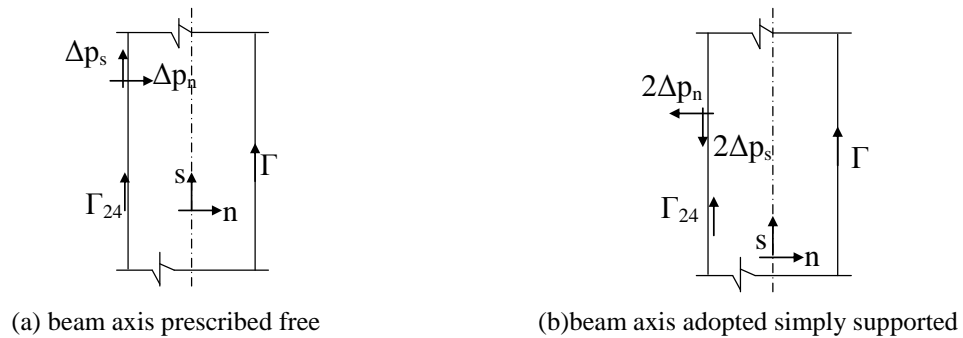For external beams, only the interface in-plane tractions have to be approximated as the

(a) beam axis prescribed free   (b) beam axis adopted simply supported

Fig. 3 Tractions acting along external beam interfaces

external boundary tractions represent the actual boundary values. In this case, the interface values Δp_n and Δp_s are also written in terms of displacements derivatives as described in Eq. (27) and the in-plane tractions approximation depends on the boundary conditions of the beam axis. They are approximated as described in Fig. 3(a) when the beam axis is prescribed free or as defined in Fig. 3(b) if the beam axis is adopted simply supported.

It is important to stress that all values are referred to nodes defined along the beam axis, while the integrals are still performed along the interfaces. Thus, no singular or hyper-singular term is found when transforming the integrals representations into algebraic ones.

4. Algebraic equations

As usual for any BEM formulation, the integral representations (Eqs. (23) and (24), as example) are transformed into algebraic expressions after discretizing the external boundary without beams and the beams axis into geometrically linear elements, where quadratic shape functions have been adopted to approximate the variables. As domain integrals in term of displacements are defined in Eq. (24) the domain has also to be discretized into cells where the displacements u_1, u_2, $w_{,1}$ and $w_{,2}$ have to be approximated.

We have adopted different kind of cells for the beams and slabs. In the beams each three nodes element defines a beam rectangular cell (see Fig. 4, where 1, 2 and 3 are the element nodes). Then each beam rectangular cell is divided into four triangular cells over which the displacements are approximated by continuous linear shape functions (see Fig. 4, where 1', 2', 3', 1", 2" and 3" are the triangular cells nodes). Then the values related to the triangular cells nodes are translated to the beam axis nodes, using the same kind of approximations defined previously along the beam cross section. Thus no additional degrees of freedom are defined in the beams, as the beam cells nodes are coincident to the beam axis nodes. To perform the integral over these triangular cells we have transformed the domain integrals into cell boundary integrals, which have been performed numerically by using a sub-element scheme that has already demonstrated to be efficient and accurate. The same kind of triangular cells have been used to discretize the slabs domain, where the displacements u_1, u_2, $w_{,1}$ and $w_{,2}$ defined in the slabs cells nodes represent new independent values.

Along the external boundary without beams the nodal values are: two in-plane displacements (u_n and u_s) for the stretching problem; one deflection w and its normal derivative $w_{,n}$ for the
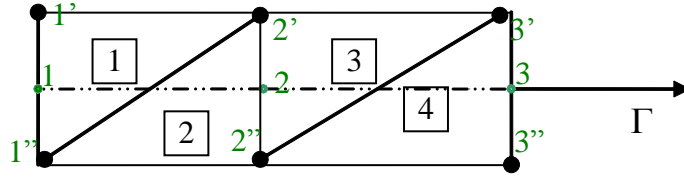
Gabriela R. Fernandes and João R. Neto

Fig. 4 Discretization of a generic beam rectangular cell into four triangular cells

bending problem. The counterpart values are respectively: in-plane tractions (p_n and p_s) for the stretching problem; bending moment M_n and the effective shear force V_n for the bending problem. Therefore, four equations must be written for each boundary node as four unknowns are defined per node. Besides, on the corners is defined the deflection w and its counterpart value given by the corner reaction R_c, requiring therefore one equation in each corner. Along the beams axis we have defined two in-plane displacements u_n and u_s, two displacement derivatives with respect to the skeleton line normal direction, $\partial u_n / \partial n$ and $\partial u_s / \partial n$ for the stretching problem, and one deflection w and one deflection derivative $w_{,n}$ for the bending problem. Besides, in the internal beams there are also the in-plane tractions p_n and p_s as unknowns. Thus, for each external and internal beams axis node, six and eight relations are required, respectively.

For each boundary node we have defined one outside collocation point very near to the boundary and another one coincident to the node. For the collocation on the boundary we write three displacements algebraic relations: two in-plane displacement relations (Eq. (24)) and one deflection relation (Eq. (23)). For the external point we write only the deflection Eq. (23). Note that we have chosen to write the deflection equation for one outside collocation point instead of employing the gradient equation because in previous studies (see Venturini and Paiva 1993, Paiva and Venturini 1992) this technique showed to lead to very good results.

For each beam skeleton node we write two in-plane displacement relations obtained from Eq. (24), one deflection relation from Eq. (23), two in-plane displacement derivative relations and one slope relation. Besides, for internal beams two in-plane traction relations have to be added. These collocations points are coincident to the node when variable continuity is assumed or defined at skeleton element internal point when variable discontinuity is required. Finally, the amount of equations required to solve the problem is completed by writing the equations of displacements u_1, u_2, $w_{,1}$ and $w_{,2}$ at the cells nodes defined in the slabs domain.

After writing the required number of algebraic equations, one can get the set of equations defined in (28) to solve the problem in terms of boundary, beam axis and slab domain values. Note that if the coupled stretching- bending problem is considered, in Eq. (28) the bending and stretching problems have to be coupled and cannot be treated separately.

$$
\begin{bmatrix}
[H]^B & [H]^c & [\overline{H}]^S & [0] \\
--- & -- & -- & -- \\
[\overline{\overline{H}}]^B & [0] & [H]^S & [E]
\end{bmatrix}
\begin{Bmatrix}
\{U\}_B \\
\{U\}_c \\
\{U\}_S \\
\{U\}_i
\end{Bmatrix}
=
\begin{bmatrix}
[G]^B & [G]^c & [\overline{G}]^S \\
--- & -- & -- \\
[0] & [0] & [G]^S
\end{bmatrix}
\begin{Bmatrix}
\{P\}_B \\
\{P\}_c \\
\{P\}_S
\end{Bmatrix}
+
\begin{Bmatrix}
\{T\}^B \\
--- \\
\{T\}^S
\end{Bmatrix}
\tag{28}
$$

In Eq. (28) the upper and bottom parts indicate, respectively, algebraic equations of the bending and stretching problems; $\{U\}$ and $\{P\}$ are displacement and traction vectors, respectively; the subscripts B and S are related to values defined on the external boundary and beam skeleton lines

(a) plate modelling for simple bending analysis

(b) plate modelling for the coupled stretching-bending problem

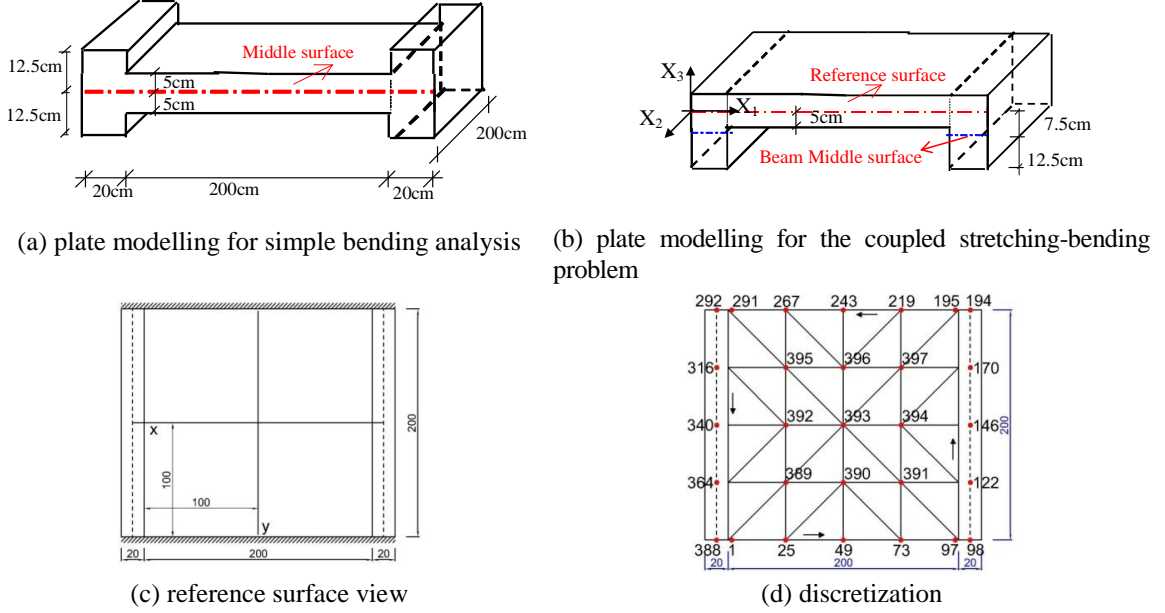(c) reference surface view

(d) discretization

Fig. 5 Plate reinforced by two external beams

of bending and stretching problems, respectively; the subscript *C* is related to the corners and *i* to the internal nodes of the slabs domain; {*T*} is the independent vector due to the applied loads; [*H*] and [*G*] are matrices obtained by integrating all boundary and interfaces and also the beams cells for the stretching equations, $[\bar{H}]^S$ and $[\bar{G}]^S$ represent the influence of the stretching problem into the bending problem; $[\bar{H}]^B$ is the influence of the bending problem into the stretching problem; [*E*] is computed by the integration of the triangular cells defined in the slabs domain.

Eq. (28) can be represented in a reduced form, as follows

$$HU = GP + T \tag{29}$$

where **U** contains the generalized displacement nodal values defined along the boundary, the skeleton lines, the corners and slabs domain; **P** contains nodal tractions on the boundary, corners and skeleton lines; **T** is the independent vector due to the applied loads.

5. Numerical applications

Two examples are now shown to demonstrate the performance of the proposed formulation being the results compared to a well-known finite element code (ANSYS, version 9), where solid elements have been adopted to analyse the coupled stretching-bending problem. Moreover results computed considering the BEM formulation presented in Fernandes (2009) are also presented in order to show the difference between the coupled stretching-bending analysis and the simple bending analysis. In the numerical analysis related to Fernandes (2009) only the beam axis and the external boundary without beams have to be discretized as there are no domain integrals involving the displacements. Observe that in the proposed model the elements placed at external beams ends,
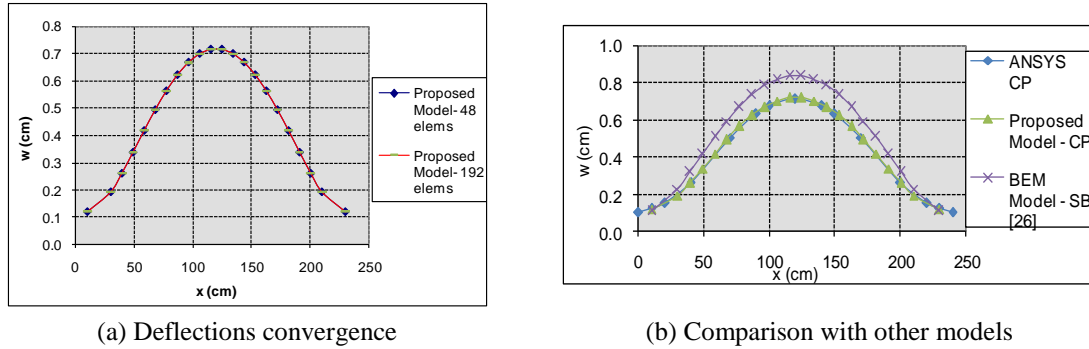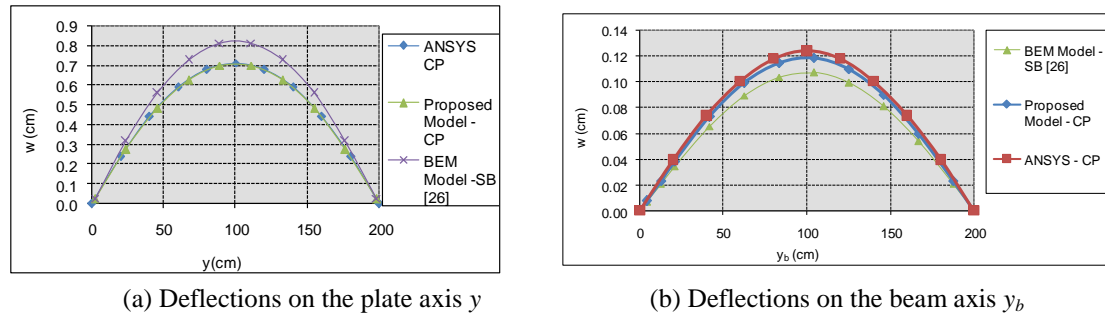
(a) Deflections convergence

(b) Comparison with other models

Fig. 6 Deflections on the plate axis *x* - Example 1

(a) Deflections on the plate axis *y*

(b) Deflections on the beam axis y_b

Fig. 7 Deflections in the stiffened plate - Example 1

in the direction of the beam width, are automatically generated by the code, so that there is no need of defining them. Besides, for all presented examples a simple convergence test has confirmed that the obtained displacements and other relevant values practically do not change when finer meshes were used leading to the same results presented herein.

In the first numerical example the plate is reinforced by two boundary beams, increasing the stiffness of the structural system mainly in the x_1 direction, as shown in Fig. 6(a), where Fig. 5(a) and 5(b) indicate how the stiffened plate is analysed, respectively, in simple bending and the coupled stretching-bending analysis. A distributed load *g* of 0.04 kN/cm^2 is applied over all surface of the stiffened plate. The two sides defined in the span direction of the beams are assumed free ($V_n=M_n=0.0$) while the other two are considered simply supported (*w=M_n=0.0*), as shown in Fig. 5(c). For this analysis thickness t_p=10.0 cm, Poisson's ratio v_p=0.2 and Young's modulus E_p=3×10^3 kN/cm^2 have been adopted for the plate, while t_b=25 cm, v_b=0.15 and E_b=2.7×10^4 kN/cm^2 have been assumed for the beams. For the coupled stretching-bending analysis, the plate middle surface has been adopted as reference surface, resulting into c_p=0.0 and c_b=7.5 cm for the plate and beam, respectively.

To verify the results convergence two discretizations have been used, adopting for both 32 cells to discretize the slab domain. In the poorest one each plate side without beams and each beam axis was discretized by 12 quadratic elements, giving the total amount of 48 elements and 100 nodes while for the finest mesh (presented in Fig. 5(d) we have adopted 192 elements with 388 nodes. The displacements along the slab axis *x* (see Fig. 5(c)) obtained with these two meshes are very similar, as one can observe in Fig. 6(a).
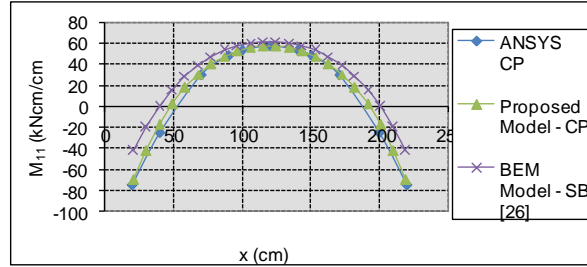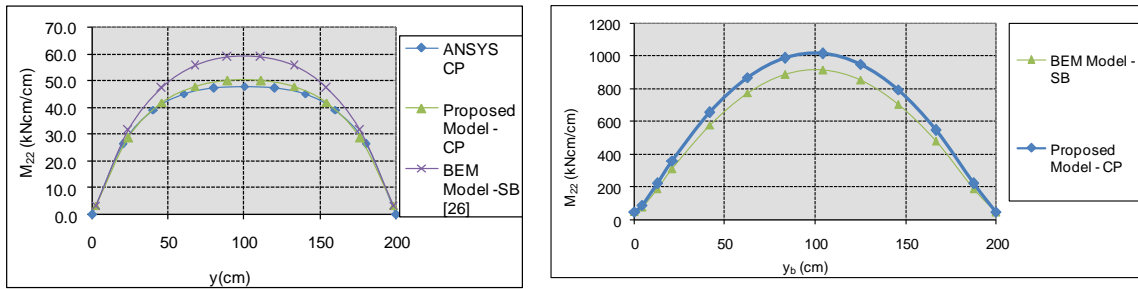
Fig. 8 Moments M_{11} on the plate middle axis *x*- Example 1

(a) Moments M_{22} on the plate axis *y*   (b)Moments M_{22} on the beam axis y_b

Fig. 9 Moments in the stiffened plate - Example 1

Deflections obtained in the plate middle axes *x* and *y* (see Fig. 5(c)) as well as along the beam axis y_b, are displayed, respectively, in Figs. 6(b), 7(a) and 7(b) where SB refers to the simple bending analysis obtained from the formulation presented in Fernandes (2009) and CP to the coupled stretching-bending problem. As can be seen the numerical results in the slabs compare very well with the ones obtained by ANSYS and the deflections along the beam axis are very similar to ANSYS.

Some moments components along the axis *x*, *y* and y_b are presented in Figs. 8, 9(a) and 9(b), respectively. As we can observe in the slabs the moments also compare very well with the ones obtained by ANSYS. Note that the moments obtained from ANSYS along the beam axis are not presented, because as the ANSYS compute only stress components is not possible to obtain the moments in the beams.

In the second example we have a building floor structure defined by five beams and two plate regions as shown in Fig. 10, where the slabs surface has been assumed as the reference surface and the length unit is centimetre. The plate thickness has been considered equal to t_p=8.0 cm while for the beams B_1 and B_2 we have adopted height t_b=25.0 cm and t_b=15.0 cm has been assumed for B_3, B_4 and B_5. Besides, it has been adopted Young's modulus E_b=25000 kN/cm^2 and E_p=3000 kN/cm^2, respectively, for the beams and plates as well as the following Poisson rations: v_b=0.3 and v_p=0.2. A distributed load of 0.003 kN/cm^2 has been applied over the whole stiffened plate surface while all plate sides are considered simply supported (note that the values $w=M_n$=0 are prescribed along the beam axis). Besides it has been prescribed in-plane tractions nulls along all external beams axis, except for nodes 71, 103 and 87 (see Fig. 10) where has been adopted u_n=0 for nodes 71 and 103 and u_s=0 for the node 87. To confirm the results convergence three meshes have been considered. The poorest one (see Fig. 10) contains 82 elements and 173 nodes defined on the
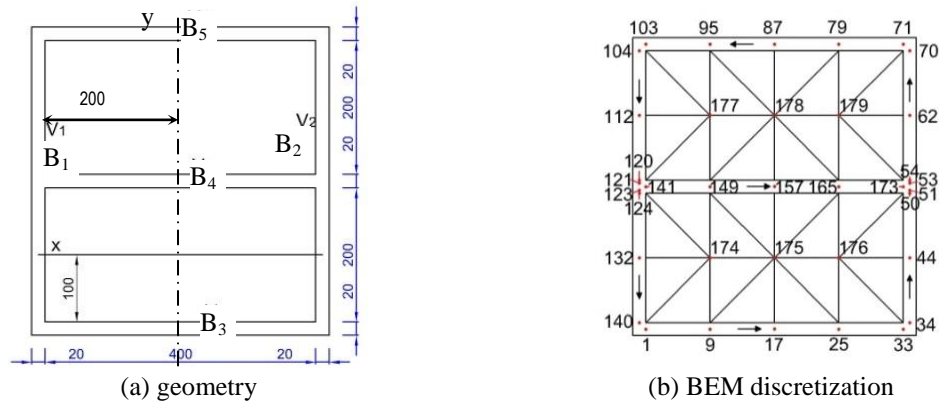
(a) geometry

(b) BEM discretization

Fig. 10 Building floor structure

(a) Deflections convergence

(b) Comparison with other models

Fig. 11 Deflections along Beam Axis X_b - Example 2

(a) Deflections along axis y

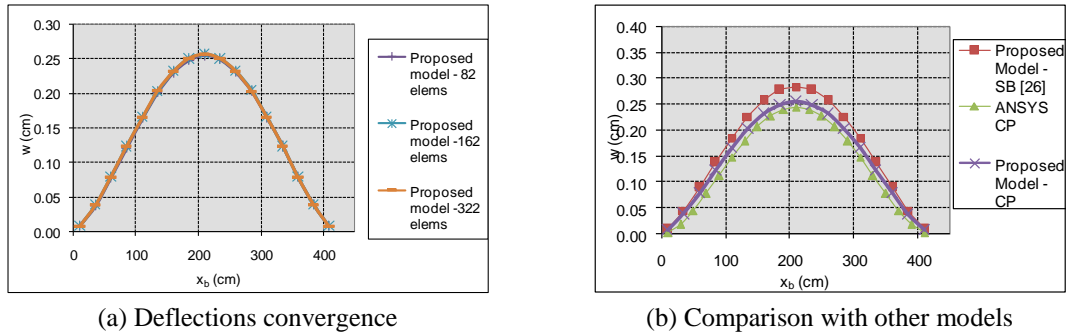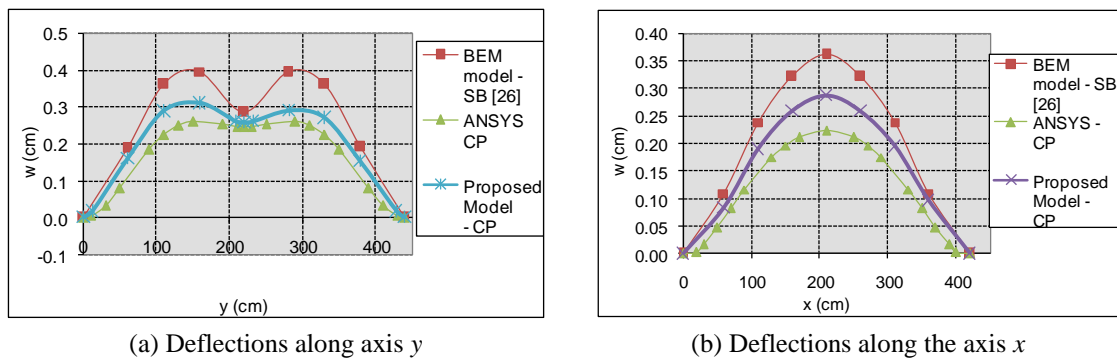(b) Deflections along the axis x

Fig. 12 Deflections in the plate- Example 2

beams axis while 16 triangular cells have been used to discretize each slab domain, resulting into 32 cells. The other two meshes (162 and 322 elements) have been obtained by doubling the number of elements of the previous mesh (except at beams intersections, where has been adopted one element). Besides, to confirm the convergence we have also considered 64 cells over the domain, but no difference was observed in the numerical results. Despite the deflections along the internal beam axes presents a very good convergence (see Fig. 11 (a)), the finer mesh had to be
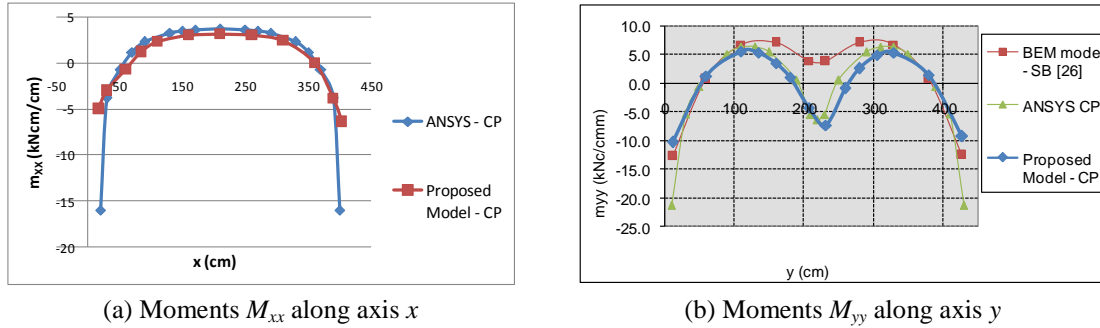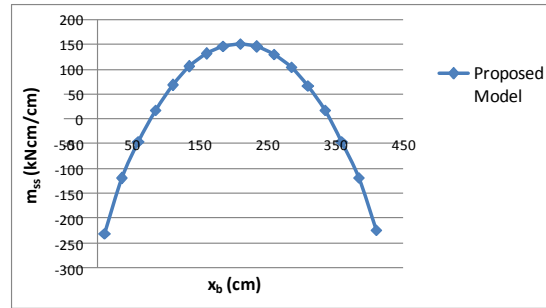
(a) Moments M_{xx} along axis x (b) Moments M_{yy} along axis y

Fig. 13 Moments in the plate - Example 2

Fig. 14 Moments M_{ss} along the internal beam axis - Example 2

considered to compute the numerical results for moments.

The deflections along the internal beam axis as well as the ones along the plate middle axes x and y defined in Fig. 10 are displayed, respectively, in Figs. 11(b), 12(a) and 12(b). As can be observed, the results along the internal beam compare very well to ANSYS. On the other hand, the deflections along the axes x and y are similar to the ones obtained with ANSYS, but a little bigger. The bending moments along the plate middle axes x and y are displayed in Figs. 13(a) and 13(b), where can be observed a good agreement with the ANSYS results. The bending moments along the internal beam axes are shown in Fig. 14, where the results are not compared to ANSYS, because is not possible to compute the moments in the beams with the stress given by ANSYS.

6. Conclusions

A BEM formulation based on Kirchhoff's hypothesis for performing the coupled stretching-bending analysis of reinforced plates has been extended to define sub-regions with different materials, i.e., different Young's modulus and Poisson's ratio. The proposed integral representations can be also used to analyse the bending and stretching problems separately without coupling them. The beams are assumed as narrow sub-regions, without dividing the reinforced plate into beam and plate elements. In the coupled stretching-bending analysis the elements are not displayed over their middle surface, i.e., eccentricity effects are taken into account. This composed structure is treated as a single body, where equilibrium and compatibility conditions are automatically guaranteed by the global integral equations. To compute the domain integrals of the

integral representation of in-plane displacements, the stiffened plate domain had to be discretized into cells where different approximations had been adopted for the displacements over the slabs and beams domain. In the beams the cells nodes are adopted coincident to the elements nodes, while the nodal values for displacements of the cells defined in the slabs domain represent new independent values. The performance of the proposed formulation has been confirmed by comparing the results with a well-known finite element code.

Acknowledgements

References

Aliabadi, M.H. (1998), *Plate Bending Analysis with Boundary Elements*, Advanced boundary elements series, Computational Mechanics Publications, Southampton.

Beskos D.E. (1991), *Boundary Element Analysis of Plates and Shells*, Springer Verlag, Berlin.

Bezine, G.P. (1981), "A boundary integral equation method for plate flexure with conditions inside the domain", *Int. J. Numer. Meth. Eng.*, **17**, 1647-1657.

Bezine, G.P. (1978), "Boundary integral formulation for plate flexure with arbitrary boundary conditions", *Mech. Res. Comm.*, **5**(4), 197-206.

Fernandes, G.R. and Venturini, W.S. (2007), "Non-linear boundary element analysis of floor slabs reinforced with rectangular beams", *Eng. Anal. Bound. Elem.*, **31**, 721-737.

Fernandes, G.R. and Venturini, W.S. (2002), "Stiffened plate bending analysis by the boundary element method", *Comput. Mech.*, **28**, 275-281.

Fernandes, G.R. (2009), "A BEM formulation for linear bending analysis of plates reinforced by beams considering different materials", *Eng. Anal. Bound. Elem.*, **33**, 1132 - 1140.

Fernandes, G.R. and Venturini, W.S. (2005), "Building floor analysis by the Boundary element method", *Comput. Mech.*, **35**, 277-291.

Fernandes, G.R., Denipotti, G.J. and Konda, D.H. (2010), "A BEM formulation for analysing the coupled stretching-bending problem of plates reinforced by rectangular beams with columns defined in the domain", *Comput. Mech.*, **45**, 523 - 539.

Hartley, G.A. (1996), "Development of plate bending elements for frame analysis", *Eng. Anal. Bound. Elem.*, **17**, 93-104.

Hu, C. and Hartley, G.A. (1994), "Elastic analysis of thin plates with beam supports", *Eng. Anal. Bound. Elem.*, **13**, 229-238.

Paiva, J.B. and Aliabadi, M.H. (2004), "Bending moments at interfaces of thin zoned plates with discrete thickness by the boundary element method", *Eng. Anal. Bound. Elem.*, **28**, 747-751.

Paiva, J.B. and Aliabadi, M.H. (2000), "Boundary element analysis of zoned plates in bending", *Comput. Mech.*, **25**, 560-566.

Paiva, J.B. and Venturini, W.S. (1992), "Alternative technique for the solution of plate bending problems using the boundary element method", *Adv. Eng. Softw.*, **14**, 265-271.

Sapountzakis, E.J. and Katsikadelis, J.T. (2000a), "Analysis of plates reinforced with beams", *Comput. Mech.*, **26**, 66-74.

Sapountzakis, E.J. and Katsikadelis, J.T. (2000b), "Elastic deformation of ribbed plates under static, transverse and inplane loading", *Comput. Struct.*, **74**, 571-581.

Sapountzakis, E.J. and Mokos V. G. (2007), "Analysis of plates stiffened by parallel beams", *Int. J. Numer.*

Meth. Eng., **70**, 1209-1240.

Stern, M.A. (1979), "A general boundary integral formulation for the numerical solution of plate bending problems", *Int. J. Solid. Struct.*, **15**, 769-782.

Tanaka, M. and Bercin, A.N. (1997), "A boundary element method applied to the elastic bending problems of stiffened plates", *Bound. Elem. Meth. XIX*, Eds. C.A. Brebbia *et al*., CMP, Southampton.

Tanaka, M., Matsumoto, T. and Oida, S. (2000), "A boundary element method applied to the elastostatic bending problem of beam-stiffened plate", *Eng. Anal. Bound. Elem.*, **24**,751-758.

Tottenhan, H. (1979), "The boundary element method for plates and shells", Developments in boundary element methods, Eds. Banerjee, P.K. and Butterfield, R., 173-205.

Venturini, W.S. and Paiva, J.B. (1993), "Boundary elements for plate bending analysis", *Eng. Anal. Bound. Elem.*, **11**, 1-8.

Venturini, W.S. and Waidemam, L. (2009a), "An extended BEM formulation for plates reinforced by rectangular beams", *Eng. Anal. Bound. Elem.*, **33**, 983-992.

Venturini, W.S. and Waidemam, L. (2009b), "BEM formulation for reinforced plates", *Eng. Anal. Bound. Elem.*, **33**, 830-836.

Waidemam, L. and Venturini, W.S. (2010), "A boundary element formulation for analysis of elastoplastic plates with geometrical nonlinearity", *Comput. Mech.*, **45**, 335-347.

Wutzow, W.W., Venturini, W.S. and Benallal, A. (2006), "BEM poroplastic analysis applied to reinforced solids", *Advances in Boundary Element Techniques*, Paris.

CC